J|A|C|S
COMMUNICATIONS

Published on Web 10/26/2004

A Trimeric HIV-1 Fusion Peptide Construct Which Does Not Self-Associate in Aqueous Solution and Which Has 15-Fold Higher Membrane Fusion Rate

Rong Yang,[†] Mary Prorok,[‡] Francis J. Castellino,[‡] and David P. Weliky*,[†]

Department of Chemistry, Michigan State University, East Lansing, Michigan 48824, and Department of Chemistry and Biochemistry and W. M. Keck Center for Transgene Research, University of Notre Dame, Notre Dame, Indiana 46556

Received July 21, 2004; E-mail: weliky@chemistry.msu.edu

Enveloped viruses such as HIV-1 are surrounded by a membrane and enter into host cells via fusion of the viral membrane with the target cell membrane.[1,2] Fusion is mediated by envelope proteins in the viral membrane which contain apolar fusion peptide (FP) domains that interact with the target cell membrane and play a key role in membrane fusion.[3] For the HIV-1 virus, the FP is the ~20 N-terminal amino acids of the gp41 envelope protein, and peptides composed of the FP sequence induce fusion between large unilamellar vesicles (LUVs) or between red blood cells.[4] There are similar mutation/fusion activity relationships for peptide-induced fusion and virus-induced fusion which suggests that the peptide by itself is a useful model system to understand some aspects of viral/target cell fusion.[3,5] There are also high-resolution structures of the gp41 "soluble ectodomain" which begins ~10 residues C-terminal of the FP.[2] Although the apolar FP is not part of the soluble ectodomain, the structures show trimeric oligomerization with the three N-termini in close proximity. These data suggest that during viral/target cell fusion, gp41 is trimeric with the C-termini of three FPs close together. In an effort to mimic the biologically relevant topology in a peptide model system, we have synthesized and functionally characterized a fusion peptide trimer (FPtr) whose three FP strands are chemically bonded at their C-termini. To assess the significance of the oligomeric topology and of trimerization, comparative measurements were made for monomeric (FPmn) and cross-linked dimeric (FPdm) peptides. The amino acid sequences of all of the peptides are displayed in Figure 1A. In addition to the native FP sequence, the peptides contain lysines in their C-terminal regions to improve aqueous solubilities and tryptophans as 280 nm chromophores.[6] One strand of FPtr also has a C-terminal β-alanine because it was included in the commercial low-substitution resin used in the synthesis.

FPdm was synthesized by cross-linking two monocysteine peptides.[7] Trimer synthesis had previously been attempted by cross-linking dicysteine and monocysteine peptides in 1:4 ratio, but as would be expected from statistics, this approach gave very high yield of dimer and very low (~1%) yield of trimer. In the present study, the trimer was synthesized with a lysine side chain scaffold and gave ~6% (0.6 μmol) purified yield. Fluorenylmethoxycarbonyl (Fmoc)-based solid-phase methods were used, and the trimer backbone was initially formed with two sequential couplings of *N*-α-Fmoc-*N*-ϵ-4-methyltrityl-L-lysine (Fmoc-Lys(Mtt)) followed by a coupling with *N*-α-Fmoc-*N*-ϵ-*tert*-butoxycarbonyl-L-lysine. Prior to the second and third couplings, the Mtt group on the lysine side chain was removed with 1% trifluoroacetic acid (TFA) in dichloromethane.[8] The rest of the trimer was then synthesized using standard Fmoc peptide chemistry followed by cleavage from the resin with 80% TFA and purification with reversed-phase HPLC.

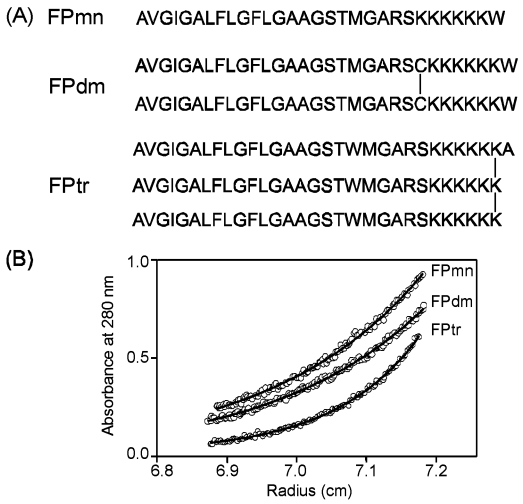

Figure 1. (A) FP constructs and (B) sedimentation equilibrium analytical ultracentrifugation data and fitting. The buffer solution was 5 mM HEPES pH 7 and the FPmn, FPdm, and FPtr concentrations were ~100, 40, and 25 μM, respectively. The fitted FPmn, FPdm, and FPtr masses in solution are 3000, 5700, and 11000 g/mol, respectively, and are close to the actual nonassociated peptide masses of 3080, 6364, and 9274 g/mol.

One goal of the present study is correlation of the different numbers of strands in FPmn, FPdm, and FPtr with their respective fusion activities. In fusion assays, FPs bind to membranes from aqueous solution, and the correlation of fusogenicity with numbers of strands could be confounded by prior self-association of FPs in aqueous solution, as has been commonly observed with other FP constructs.[7,9] Figure 1B displays analytical ultracentrifugation data for the present study's constructs at concentrations comparable to those of functional assay stock solutions. The fitted masses in solution are close to the masses of nonself-associated FPs. To our knowledge, this is the first demonstration of a homologous series of nonself-associated FPmn, FPdm, and FPtr constructs.

The fusion activities of the different constructs were assessed using a fluorescence assay which probed FP-induced mixing of lipids between different LUVs.[10] Lipid mixing represents one of the steps in viral/target cell membrane fusion. Mixing was probed with LUVs of two different lipid compositions: (1) PC/PG-POPC and POPG in a 4:1 mol ratio; and (2) LM3-POPC, POPE, POPS, PI, sphingomyelin, and cholesterol in a 10:5:2:2:1:10 mol ratio. PC/PG has been a common composition used in studies of FPs, and LM3 reflects the approximate lipid headgroup and cholesterol composition of membranes of host cells of the virus.[11] In addition, solid-state NMR structural measurements are consistent with predominant helical conformation for PC/PG-associated FPs and with predominant β-strand conformation for LM3-associated FPs. For example, the Phe-8 ^{13}C carbonyl shift for FPtr is ~178 ppm in

[†] Michigan State University.
[‡] University of Notre Dame.

10.1021/ja045612o CCC: $27.50 © 2004 American Chemical Society

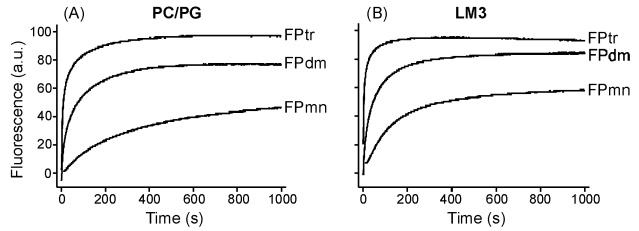

Figure 2. Stopped-flow fluorescence data for FP-induced lipid mixing in (A) PC/PG and (B) LM3 vesicles at 37 °C and [total lipid] = 150 μM, [FPmn] = 1.5 μM, FPdm = 0.75 μM, and FPtr = 0.50 μM.

Table 1. Kinetic Parameters of FP-Induced Vesicle Fusion[a]

	PC/PG			LM3		
	FPmn	FPdm	FPtr	FPmn	FPdm	FPtr
k (10^{-3} s^{-1})	13	63	190	11	76	430
E_a (kJ/mol)	54(7)	48(3)	27(1)	n.d.	n.d.	33(2)
ln A	17(3)	16(1)	9(1)	n.d.	n.d.	12(1)
$\Delta S^{\ddagger}$ (J/mol-K)	−120	−130	−190	n.d.	n.d.	−160

[a] The listed k and $\Delta S^{\ddagger}$ values are at 37 °C. Each k value has ±20% uncertainty, and the fitting uncertainties in E_a and ln A are given in parentheses. n.d. ≡ not determined because of significant uncertainties in Arrhenius fitting parameters (see Supporting Information).

PC/PG and ~173 ppm in LM3, which are consistent with helical and β-strand conformations, respectively.[12] The NMR samples were prepared under conditions similar to the fusion assays, and there was approximately quantitative binding of the FPs to membranes in these samples.

Figure 2 displays stopped-flow fluorescence data for FP-induced lipid mixing. In the assays, [FPmn] = 2[FPdm] = 3[FPtr], and the strand concentration was constant among the different constructs. The long-time changes in fluorescence are ordered $\Delta F_{mn} < \Delta F_{dm} < \Delta F_{tr}$, which suggests that the oligomeric constructs induce more vesicle fusion than FPmn. Because an increased fusion rate is likely the most important FP effect in viral/target cell fusion, the kinetics of the stopped-flow fluorescence data were analyzed to determine the variation of fusion rate with FP construct. In a single data set, the initial increase in fluorescence could be modeled by a dominant fast exponential buildup, while at longer time, there was an additional contribution from a slower buildup. The fast component likely represents the lipid mixing induced by initial interaction of FPs with membranes, and the values of its rate constant are listed in Table 1. For both PC/PG and LM3 vesicles, $k_{tr} > k_{dm} > k_{mn}$ with $k_{tr} \approx 15k_{mn}$ for PC/PG and $k_{tr} \approx 40k_{mn}$ for LM3. Thus, there is very significant correlation of the fusion rate with both the oligomeric topology enforced by C-terminal cross-linking and with the number of FP strands in the construct. Vesicle fusion does not appear to be diffusion-limited, as the k values are at most several percent of the vesicle collision rate.[13]

In an Arrhenius model, $k = A\, e^{-E_a/RT}$, and the variations in rate constants would have contributions from differences in activation energy E_a and differences in preexponential factor A. To quantify these contributions, assays and kinetic analyses were carried out over a temperature range of 25−40 °C. As displayed in Table 1, Arrhenius plots of the data yielded values of E_a and ln A for FP-induced lipid mixing in PC/PG and LM3. The values of E_a and ln A are similar for FPtr-induced fusion of either PC/PG or LM3 LUVs, and in PC/PG, $E_{a-tr} < E_{a-dm}$, E_{a-mn}, and $A_{tr} < A_{dm}$, A_{mn}. Thus, the changes in E_a and A appear to have competing effects on the magnitude of k. The entropy of activation $\Delta S^{\ddagger}$ at 37 °C was approximately calculated with the transition-state theory expression $\Delta S^{\ddagger} = R[\ln(Ah/k_BT) - 2]$ where R, h, and k_B are the standard physical constants.[14] It is not yet clear why $\Delta S^{\ddagger} < 0$ for all constructs and why $\Delta S_{tr}{}^{\ddagger} < \Delta S_{dm}{}^{\ddagger}$, $\Delta S_{mn}{}^{\ddagger}$.

In summary, enforcement of the trimeric biological FP strand topology by cross-linking reduces E_a and increases the fusion rate by a factor of 15−40. The effect is observed both for PC/PG and for LM3 fusion in which the membrane-associated FPs have dominant helical and β-strand conformations, respectively. For FPdm or FPtr in either conformation, one reason for the fusogenic enhancement may be placement of the apolar N-terminal regions of strands on one end of the oligomer and placement of the more polar C-terminal regions of strands on the other end of the oligomer. FPtr likely has the largest apolar volume which may correlate with the greatest membrane disruption and fusion rate for this construct. Fusion may also be enhanced by the larger localized free energy released upon membrane binding of multiple FP strands in FPdm and FPtr. We note that enhanced fusion has also been observed with influenza protein constructs which likely contain FPs in the biologically relevant trimeric topology.[15]

Because it is possible to obtain FPtr in ~0.5 μmol quantities and because it has negligible self-association in aqueous solution, it should be possible to study its structural and motional properties in aqueous, detergent, and membrane environments with a variety of biophysical methods. These studies should provide further insight into its enhanced fusion rate. The synthetic approach should also be applicable to fusion peptides from other viruses and perhaps to other membrane-associated peptides derived from proteins of known oligomeric stoichiometry.

Acknowledgment. This work was supported by NIH. We acknowledge assistance from Zhaoxiong Zheng, Michele Bodner, Rhonda Husain, Dr. Honggao Yan, and Dr. Ned Jackson.

Supporting Information Available: Detailed descriptions of the FPtr synthesis, analytical ultracentrifugation experiments, and lipid mixing assays and analyses including full chemical names of lipids; circular dichroism data and solid-state NMR spectra. This material is available free of charge via the Internet at http://pubs.acs.org.

References

(1) Hernandez, L. D.; Hoffman, L. R.; Wolfsberg, T. G.; White, J. M. *Annu. Rev. Cell Dev. Biol.* **1996**, *12*, 627−661.
(2) Eckert, D. M.; Kim, P. S. *Annu. Rev. Biochem.* **2001**, *70*, 777−810 and references therein.
(3) Durell, S. R.; Martin, I.; Ruysschaert, J.-M.; Shai, Y.; Blumenthal, R. *Mol. Membr. Biol.* **1997**, *14*, 97−112.
(4) (a) Freed, E. O.; Myers, D. J.; Risser, R. *Proc. Natl. Acad. Sci. U.S.A.* **1990**, *87*, 4650−4654. (b) Mobley, P. W.; Lee, H. F.; Curtain, C. C.; Kirkpatrick, A.; Waring, A. J.; Gordon, L. M. *Biochim. Biophys. Acta* **1995**, *1271*, 304−314. (c) Pereira, F. B.; Goñi, F. M.; Muga, A.; Nieva, J. L. *Biophys. J.* **1997**, *73*, 1977−1986.
(5) (a) Freed, E. O.; Delwart, E. L.; Buchschacher, G. L., Jr.; Panganiban, A. T. *Proc. Natl. Acad. Sci. U.S.A.* **1992**, *89*, 70−74. (b) Pereira, F. B.; Goñi, F. M.; Nieva, J. L. *FEBS Lett.* **1995**, *362*, 243−246. (c) Kliger, Y.; Aharoni, A.; Rapaport, D.; Jones, P.; Blumenthal, R.; Shai, Y. *J. Biol. Chem.* **1997**, *272*, 13496−13505.
(6) Han, X.; Tamm, L. K. *Proc. Natl. Acad. Sci. U.S.A.* **2000**, *97*, 13097−13102.
(7) Yang, R.; Yang, J.; Weliky, D. P. *Biochemistry* **2003**, *42*, 3527−3535.
(8) Aletras, A.; Barlos, K.; Gatos, D.; Koutsogianni, S.; Mamos, P. *Int. J. Pept. Protein Res.* **1995**, *45*, 488−496.
(9) Yang, J.; Prorok, M.; Castellino, F. J.; Weliky, D. P. *Biophys. J.* **2004**, *87*, 1951−1963.
(10) Struck, D. K.; Hoekstra, D.; Pagano, R. E. *Biochemistry* **1981**, *20*, 4093−4099.
(11) Aloia, R. C.; Tian, H.; Jensen, F. C. *Proc. Natl. Acad. Sci. U.S.A.* **1993**, *90*, 5181−5185.
(12) Zhang, H.; Neal, S.; Wishart, D. S. *J. Biomol. NMR* **2003**, *25*, 173−195.
(13) Steinfeld, J. I.; Francisco, J. S.; Hase, W. L. *Chemical Kinetics and Dynamics*; Prentice Hall: Upper Saddle River, NJ, 1999; p 131.
(14) McQuarrie, D. A.; Simon, J. D. *Physical Chemistry: A Molecular Approach*; University Science Books: Sausalito, CA, 1997; p 1168.
(15) (a) Epand, R. F.; Macosko, J. C.; Russell, C. J.; Shin, Y.-K.; Epand, R. M. *J. Mol. Biol.* **1999**, *286*, 489−503. (b) Lau, W. L.; Ege, D. S.; Lear, J. D.; Hammer, D. A.; DeGrado, W. F. *Biophys. J.* **2004**, *86*, 272−284.

JA045612O

Supporting Information for:

A Trimeric HIV-1 Fusion Peptide Construct Which Does Not Self-Associate in Aqueous Solution and Which Has Fifteen-Fold Higher Membrane Fusion Rate

Rong Yang,[†] Mary Prorok,[‡] Francis J. Castellino,[‡] and David P. Weliky[*,†]

[†]*Michigan State University, Department of Chemistry, East Lansing MI 48824 and* [‡]*University of Notre Dame, Department of Chemistry and Biochemistry and W. M. Keck Center for Transgene Research, Notre Dame, IN 46556*

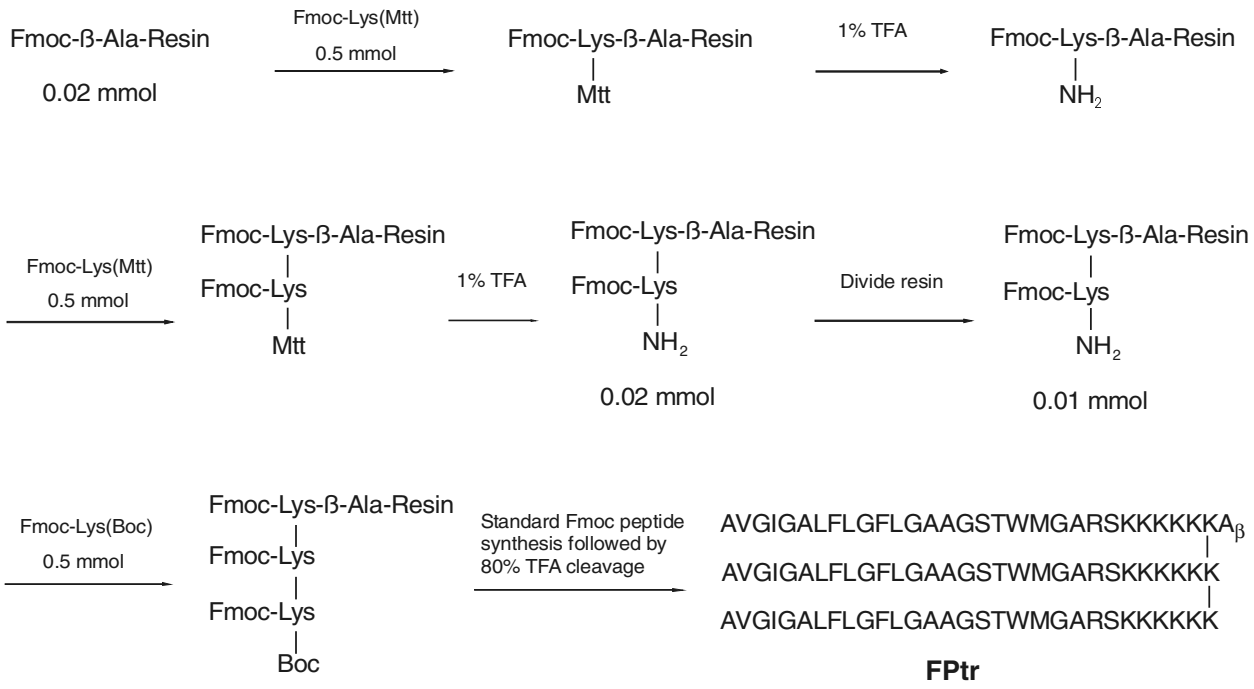

Figure S1*. FPtr synthesis scheme.*

FPtr Synthesis

N-α-Fluorenylmethoxycarbonyl-N-ε-4-methyltrityl-L-lysine (Fmoc-Lys(Mtt)) was purchased from Calbiochem-Novabiochem (La Jolla, CA) and N-α-Fmoc-N-ε-t-butoxycarbonyl-L-lysine (Fmoc-Lys(Boc)) and other Fmoc amino acids and Fmoc-β-Ala-Wang resin were purchased from Peptides International (Louisville, KY). The Fmoc-β-Ala-Wang resin was chosen because it was commercially available at lower substitution and this lower substitution may enhance yield by minimization of peptide crowding. As displayed in Fig. S1, the trimer

scaffold was made with coupling through amino groups on lysine sidechains (Aletras, A.; Barlos, K.; Gatos, D.; Koutsogianni, S.; Mamos, P. *Int. J. Pept. Protein Res.* **1995**, *45*, 488-496, and Novabiochem catalog and peptide synthesis handbook). Each Fmoc-Lys(Mtt) was added in a two hour coupling step using a peptide synthesizer (ABI 431A, Foster City, CA) and the standard Fmoc chemistry for the instrument. After each addition, the resin was taken out of the synthesizer reaction vessel and the Mtt protecting group on the lysine sidechain was removed by gentle mixing in 4 mL of a 1:5:94 mixture of trifluoroacetic acid (TFA):triisopropylsilane (TIS):dichloromethane (DCM). The mixing in the 1% TFA solution was done for two minutes and was followed by removal of the solution by filtration and a resin wash with DCM. The 1% TFA reaction/filtration/DCM wash cycle was repeated six times. The clear TFA solution became yellow when added to the resin and this yellow color was less intense with each subsequent cycle.

After addition of each Fmoc-Lys(Mtt) and removal of its Mtt group, the trimer scaffold was completed by addition of Fmoc-Lys(Boc) on the peptide synthesizer with standard Fmoc chemistry and two hour coupling time. FPtr synthesis was then continued on the synthesizer using standard chemistry and included addition of non-native lysines to improve aqueous solubility and tryptophans as 280 nm chromophores for peptide quantitation. Each amino acid was coupled for four hours and coupling was followed by acetylation of free NH_2 groups to terminate any unreacted strands. The isotopically labeled amino acids 1-^{13}C Fmoc-Phe and ^{15}N Fmoc-Leu were incorporated into the peptide at Phe-8 and Leu-9, respectively. After completion of the synthesis, peptides were cleaved from the resin in a three hour reaction using a mixture of TFA:H_2O:phenol:thioanisole:ethanedithiol in a 33:2:2:2:1 ratio. Peptides were subsequently purified by reversed-phase HPLC using a C_{18} column (Vydac, Hesperia, CA) and a

water:acetonitrile gradient which varied from 80:20 to 20:80 ratios. FPtr eluted at ~30:70 ratio and was identified by mass spectroscopy. An additional peak with +128 mass units was also observed in the FPtr mass spectrum. We believe that this peak was due to peptides which had an additional lysine on one strand. It has recently been reported that the free ε-NH_2 group of a Lys residue can catalyze the removal of the Lys Fmoc group, and in the FPtr synthesis, this premature Fmoc removal could allow coupling of an additional Lys on the first or second strand (Farrera-Sinfreu, J.; Royo, M.; Albericio, F. *Tetrahedron Lett.* **2002**, *43*, 7813-7815). Premature removal of the Fmoc group on the first Lys might also lead to formation of a peptide tetramer but there was at most a minor (<15%) peak in the tetramer region of the FPtr mass spectrum. In future FPtr syntheses, premature removal of the Fmoc group will be minimized with use of the straightforward Mtt deprotection and coupling protocol from the Albericio *Tetrahedron Lett.* paper.

Analytical Ultracentrifugation

Sedimentation equilibrium experiments at room temperature were performed on an analytical ultracentrifuge (Beckman XL-I, Palo Alto, CA) using a An-60 Ti rotor. The instrument was operated in absorbance mode at 280 nm. Samples were loaded into six-channel epon charcoal-filled centerpieces equipped with quartz windows and were equilibrated at rotor speeds of 32000, 45000, or 52000 rpm. Data were fitted with the analysis software supplied by Beckman and used a single-species model, a partial specific volume for the peptide calculated from the mass average of the partial specific volumes of the individual amino acids in the peptide, and a buffer density of 1.0 g/mL. For each fit, the residual differences between the calculated and fitted absorbances were randomly distributed around zero with typical magnitudes less than 0.02.

Lipid Mixing Assay

Preparation of large unilamellar vesicles (LUVs). Lipids and cholesterol were purchased from Avanti (Alabaster, AL). LUVs were prepared with one of two compositions: (1) "PC/PG" – 1-palmitoyl-2-oleoyl-*sn*-glycero-3-phosphocholine (POPC) and 1-palmitoyl-2-oleoyl-*sn*-glycero-3-[phospho-*rac*-(1-glycerol)] (POPG) in a 4:1 mol ratio. (2) "LM3" – POPC, 1-palmitoyl-2-oleoyl-*sn*-glycero-3-phosphoethanolamine (POPE), 1-palmitoyl-2-oleoyl-*sn*-glycero-3-[phospho-L-serine] (POPS), sphingomyelin, phosphatidylinositol (PI) and cholesterol in a 10:5:2:2:1:10 mol ratio, which reflects the approximate lipid headgroup and cholesterol composition of host cells of the HIV-1 virus (Aloia, R.C.; Tian, H.; Jensen, F. C. *Proc. Natl. Acad. Sci. U.S.A.* **1993**, *90*, 5181-5185). For either composition, ten percent of the LUVs were prepared with an additional 2 mol% of the fluorescent lipid *N*-(7-nitro-2,1,3-benzoxadiazol-4-yl)-phosphatidylethanolamine (*N*-NBD-PE) and 2 mol% of the quenching lipid *N*-(lissamine Rhodamine B sulfonyl)-phosphatidylethanolamine (*N*-Rh-PE).

LUV preparation began with cosolubilization of lipid and cholesterol in chloroform followed by removal of the chloroform with nitrogen gas and overnight vacuum pumping. A lipid dispersion was then formed with addition of pH 7 buffer containing 5 mM N-2-hydroxyethylpiperazine-N′-2-ethanesulfonic acid (HEPES) and 0.01% NaN_3 preservative. After homogenization of the dispersion with ten freeze-thaw cycles, LUVs were prepared by extrusion through a polycarbonate filter with 100 nm diameter pores (Hope, M. J.; Bally, M. B.; Webb, G.; Cullis, P. R. *Biochim. Biophys. Acta.* **1985**, *812*, 55-65).

Fluorescence assays and analyses. One feature of vesicle fusion is mixing of lipids between different vesicles. FP-induced lipid mixing between fluorescently labeled and unlabeled LUVs results in a larger distance between fluorescent and quenching lipids which can be detected as increased fluorescence (Struck, D. K.; Hoekstra, D.; Pagano, R. E. *Biochemistry* **1981**, *20*, 4093-

4099). In the assay, fluorescence was recorded on a stopped-flow fluorimeter (Applied Photophysics SX.18MV-R, Surrey, UK) using excitation and emission wavelengths of 465 and 530 nm, respectively. In the instrument, one syringe contained a mixture of labeled and unlabeled LUVs at 1:9 ratio and 300 μM total lipid concentration, and the other syringe contained FPmn, FPdm, or FPtr at 3, 2, or 1 μM concentration, respectively, as determined from 280 nm absorbance. The buffer in each syringe solution was 5 mM HEPES pH 7 with 0.01% NaN_3. Time zero in the assay was set by the ~5 ms mixing of the two solutions and fluorescence was then measured every second for ~1000 s. The temperature of the system was set to a value specified between 25 and 40 ^oC.

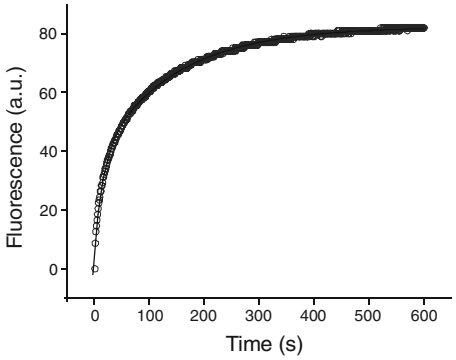

Figure S2. *Fluorescence data and fitting for FPdm-induced PC/PG lipid mixing at 37 ^oC. The step-like features at longer times are due to the digitization of the data.*

As displayed in Fig. S2, fluorescence data F(t) in arbitrary units were fitted with Eq. 1:

$$F(t) = F_0 + F_1(1 - e^{-k_1 t}) + F_2(1 - e^{-k_2 t}) \qquad (1)$$

where F_0, F_1, F_2, k_1, and k_2 are fitting parameters. F_0 represents the fluorescence intensity prior to mixing the LUV and FP solutions. The fluorescence increase after mixing was modeled as the sum of a fast buildup with overall fluorescence change F_1 and rate constant k_1, and a slow buildup with overall fluorescence change F_2 and rate constant k_2. Fitting was much poorer with a

single buildup model. In a single data set, the best-fit values of F_1 and F_2 are generally comparable, and the best-fit $k_1 \sim 10\ k_2$. The fast component likely represents the lipid mixing induced by initial interaction of FPs with membranes and the associated k_1 rate constants are listed as the rate constants k in Table 1 of the communication. The origin of the slow component in fluorescence buildup is not yet understood.

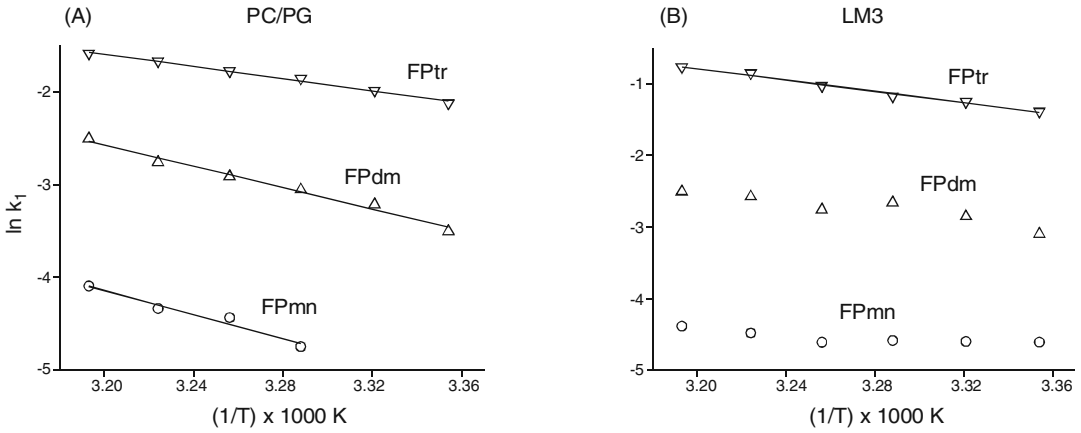

Figure S3. *Arrhenius plots for FP-induced lipid mixing in (A) PC/PG and (B) LM3.*

Fig. S3 displays k_1 Arrhenius plots and linear fits for some of the plots. The PC/PG k_2 Arrhenius plots (not shown) were also linear with trends $E_{a\text{-}tr} < E_{a\text{-}dm} < E_{a\text{-}mn}$ and $\ln A_{tr} < \ln A_{dm} < \ln A_{mn}$, which are similar to the trends observed for the PC/PG k_1 Arrhenius plots. Linear Arrhenius fitting did not appear to be very robust for FPmn and FPdm-induced fusion of LM3 vesicles, as judged by significant changes in best-fit E_a's and lnA's when different subsets of data points were fitted.

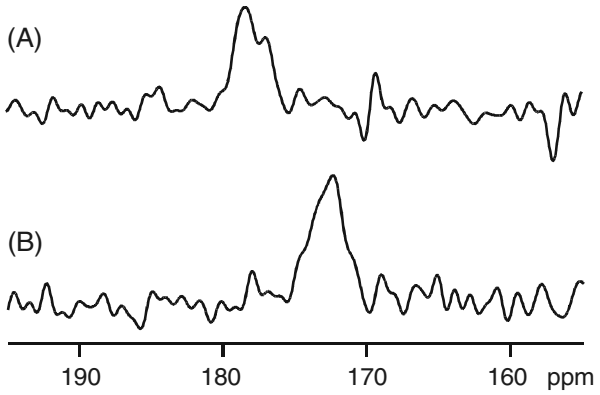

Figure S4. *Solid-state NMR spectra of FPtr in (A) PC/PG and (B) LM3.*

Circular Dichroism and Solid-State NMR Spectra

Circular dichroism spectra were obtained for FPmn, FPdm, and FPtr at ~30, 20, and 10 μM concentrations, respectively, in aqueous solution. All of the spectra had similar appearances in the 200 to 250 nm wavelength range and appear to be more characteristic of a random coil conformation than either α helical or β sheet conformation. For example, the experimental value of the mean-residue-molar-ellipticity at 220 nm (θ_{220}) is ~ +1000 deg-cm^2/dmol, and is different from the large negative (~ -20000 deg-cm^2/dmol) values characteristic of α helical or β sheet structure (Cantor, C. R.; Schimmel, P. R. *Biophysical Chemistry Part II: Techniques for the Study of Biological Structure and Function*; W. H. Freeman: New York, 1980; p. 427).

Fig. S4 displays ^{13}C solid-state NMR spectra of FPtr which was ^{13}C carbonyl labeled at Phe-8 and ^{15}N labeled at Leu-9 and bound to (A) PC/PG or (B) LM3 membranes. FPtr (~0.05 μmol) was initially dissolved in 2 mL buffer (5 mM HEPES pH 7) and then mixed with 2 mL buffer which contained LUVs (15 μmol total lipid). After overnight binding, the mixture was ultracentrifuged at 35000 rpm for 4 hours and the membrane pellet with bound FPtr was transferred to a NMR rotor. The pellet volume was ~50 μL and the final concentrations of FPtr

and total lipid in the pellet were ~1 mM and ~300 mM, respectively. The NMR spectra were obtained on a 9.4 T instrument (Varian Infinity Plus, Palo Alto, CA) with 8 kHz magic angle spinning and –50 ^{o}C temperature. REDOR subtraction was applied so that natural abundance ^{13}C signals were suppressed, and the displayed spectra are dominated by the labeled Phe-8 carbonyls (Yang, J.; Parkanzky, P. D.; Bonder, M. L.; Duskin, C. A.; Weliky, D. P. *J. Magn. Reson.* **2002**, *159*, 101-110). The spectra are externally referenced to the methylene carbon of adamantane at 40.5 ppm which corresponds to the ^{13}C referencing used in liquid-state NMR of soluble proteins (Morcombe, C. R.; Zilm, K. W. *J. Magn. Reson.* **2003**, *162*, 479-486). Each spectrum represents ~120,000 scans. The motivation for use of low temperature was the three-fold higher signal-to-noise at –50 ^{o}C relative to 25 ^{o}C. A previous solid-state NMR study also showed that the ^{13}C chemical shifts of membrane-associated FPs vary little over this temperature range (Bodner, M. L.; Gabrys, C. M.; Parkanzky, P. D.; Yang, J.; Duskin, C. A.; Weliky, D. P. *Magn. Reson. Chem.* **2004**, *42*, 187-194).